Published in final edited form as:

Nature. 2010 May 27; 465(7297): 435–440. doi:10.1038/nature09032.

G domain dimerization controls dynamin's assembly-stimulated GTPase activity

Joshua S. Chappie[1,2], **Sharmistha Acharya**[2], **Marilyn Leonard**[2], **Sandra L. Schmid**[2], and **Fred Dyda**[1]

[1]Laboratory of Molecular Biology, National Institute of Diabetes and Digestive and Kidney Diseases, NIH, Bethesda, MD 20892, USA.

[2]Department of Cell Biology, The Scripps Research Institute, La Jolla, CA 92037, USA.

Abstract

Dynamin is an atypical GTPase that catalyzes membrane fission during clathrin-mediated endocytosis. The mechanisms of dynamin's basal and assembly-stimulated GTP hydrolysis are unknown, though both are indirectly influenced by the GTPase effector domain (GED). Here we present the 2.0Å resolution crystal structure of a minimal GTPase-GED fusion protein (GG) constructed from human dynamin 1, which has dimerized in the presence of the transition state mimic GDP.AlF_4^-. The structure reveals dynamin's catalytic machinery and explains how assembly-stimulated GTP hydrolysis is achieved through G domain dimerization. A sodium ion present in the active site suggests that dynamin uses a cation to compensate for the developing negative charge in the transition state in the absence of an arginine finger. Structural comparison to the rat dynamin G domain reveals key conformational changes that promote G domain dimerization and stimulated hydrolysis. The structure of the GG dimer provides new insight into the mechanisms underlying dynamin-catalyzed membrane fission.

Dynamin, which catalyzes membrane fission during clathrin-mediated endocytosis1, is the prototypical member of a family of large GTPases that share the common properties of low affinity for guanine nucleotides, high basal turnover, and the propensity for oligomerization into helical arrays2. Purified dynamin tetramers3 exhibit basal GTPase activity, which is stimulated >100-fold by self-assembly into helical arrays on negatively charged lipid templates4. GTP hydrolysis is required for dynamin-catalyzed membrane fission *in vivo*4–7 and in vitro8, yet paradoxically causes disassembly of dynamin helices and dissociation of dynamin subunits from the membrane 8–11. The underlying mechanisms of dynamin's basal

Correspondence and requests for materials should be addressed to S.L.S. (slschmid@scripps.edu) or F.D. (dyda@helix.nih.gov).

Supplementary Information accompanies the paper on www.nature.com/nature

Author Contributions J.S.C. designed, purified, and characterized all GG proteins and crystallized the GG dimer. J.S.C. and F.D. collected x-ray diffraction data and solved the structures. S.A. and M.L. purified full-length dynamin constructs and carried out biochemical assays. J.S.C., S.L.S, and F.D. designed experiments and interpreted data. J.S.C, S.L.S. and F.D. prepared the manuscript.

Author Information The atomic coordinates of the GG long axis and short axis dimers are deposited in the Protein Data Bank with accession numbers 2×2e and 2×2f respectively. Reprints and permissions information is available at www.nature.com/reprints. The authors declare no competing financial interests.

and assembly-stimulated activities are unknown and its catalytic machinery has yet to be identified.

Dynamin consists of five domains (Supplementary Fig. 1a), including: an N-terminal G domain that binds and hydrolyzes GTP, a middle domain involved in self-assembly and oligomerization, a pleckstrin homology (PH) domain responsible for interactions with the plasma membrane, GED, which is also involved in self-assembly, and a proline arginine rich domain (PRD) that interacts with SH3 domains on accessory proteins1,2. While a high-resolution structures showing the organization of these domains does not yet exist, models based on low resolution cryo-electron microscopy (cryo-EM) structures suggest that the middle domain and GED form a coiled-coil 'stalk' that connects the membrane-bound PH domain 'leg' to the GTPase 'head'12,13 (Supplementary Fig. 1b). Mutagenesis has established the importance of this middle/GED stalk in stabilizing higher-ordered dynamin assemblies 14–16.

GED mutations also impair both assembly-stimulated14,17–19 and basal14,18 GTP hydrolysis, leading in some cases to enhanced rates of endocytosis17,18. Two-hybrid analysis20 and the crystal structures of the rat dynamin21 and Dictyostelium dynamin A22 G domains have suggested that GED might associate directly with the G domain. We previously confirmed this by engineering a minimal GTPase-GED fusion protein (GG)19 that connects residues 6–320 and residues 726–750 from human dynamin 1 via a flexible linker (Fig. 1a). The resulting 39.3 kDa construct recapitulated dynamin's basal hydrolysis19, suggesting that it encodes the fundamental catalytic machinery. We therefore utilized GG to dissect the mechanisms of dynamin GTP hydrolysis.

The structure of an activated GG dimer

GG elutes as a monomer in the absence of nucleotides (Supplementary Fig. 2). This behavior is unaltered by the addition of GDP or non-hydrolyzable GTP analogs. However, GG dimerizes when incubated with either GTP or GDP in the presence of NaF and $AlCl_3$. The requirement for the transition state mimic GDP.AlF_4^- suggests that dimerization is important for the activation of dynamin's GTPase domain.

To elucidate the role of G domain dimerization in GTP hydrolysis, we solved the structure of the GDP.AlF_4^- -stabilized GG dimer by X-ray crystallography in two crystal forms: a "long axis" form (Fig. 1) and a "short axis" form (Supplementary Table 1 and Methods). In each of these structures, the GG dimer is two-fold symmetric and is formed through the association of the individual GTPase cores (residues 32–292), which buries a surface area of 2561Å^2 for the long axis form (Fig. 1b) and 2569Å^2 for the short axis form. The active sites of each monomer are positioned close to the dimer interface with the bound nucleotides oriented in a parallel fashion relative to one another.

Three key intermolecular interactions contribute to the GG dimer interface. The first involves the dual coordination of the guanine base both *in cis* and *in trans* by the G4 loop (residues 205–216) (Fig. 1c), which contains the conserved G4 element (^{205}TKLD^{208}) that imparts nucleotide specificity via D208's interaction with the guanine base *in cis*. Upon dimerization, D211 from the adjacent monomer forms two additional hydrogen bonds with

the guanine base *in trans* at positions 2 and 3. Concomitantly, D211 and E212 interact with Q239 and K240 across the dimer interface, partially stabilizing the conformation of residues 236–246, designated the "dynamin specific loop" (DSL). Together these elements form a lid at the top of the dimer that caps the active sites. The second is the association of switch II (residues 136–153) with the "*trans* stabilizing loop" (residues 176–188) (Fig. 1d), mediated primarily by main chain interactions, and bolstered by interactions between V145 of switch II and leucines 224 and 225 (the "LL patch") and by hydrogen bonding between N183 and the main chain atoms of Q40 in the P-loop. These segments represent the bulk of the buried surface between the two monomers. The final stabilizing component is a pair of symmetric salt bridges between E153 and K188 that anchor the base of the dimer *in trans* (Fig. 1e). K142 forms an *in cis* hydrogen bond with E153 that complements this interaction.

The catalytic machinery of dynamin GTP hydrolysis

Efficient GTP hydrolysis requires 1) the correct positioning of a water molecule for a nucleophilic attack on the γ-phosphate, 2) neutralization of a negative charge that develops between the β- and γ-phosphates in the transition state, and 3) stabilization of the conformationally flexible switch regions within the catalytic core23,24. These conditions are achieved either through interaction with a GTPase-activating protein (GAP)25,26 or through dimerization27. The GG dimer structure reveals how dynamin accomplishes these requirements.

In the active site of each GG monomer, the main chain carbonyl of T65 and the backbone nitrogen of G139 position the catalytic water in line with the AlF_4^- moiety (Fig. 2a). A second water molecule further orients the catalytic water by acting as a bridge to the Q40 side chain and the G139 carbonyl oxygen. This type of indirect positioning has thus far only been observed in the tRNA modifying MnmE GTPase28. D180 of the *trans* stabilizing loop reaches across the dimer interface and forms hydrogen bonds with Q40, S41, and the main chain nitrogen of G62 (Fig. 2a). These interactions stabilize the P-loop and switch I conformations such that they are poised for catalysis.

Notably absent from the GG active site is a charge-compensating arginine finger. Instead, we observe additional electron density that we interpreted as a sodium ion (Supplementary Fig. 3a). The ligands for this ion include the aluminum fluoride, b-phosphate, carbonyl oxygens of G60 and G62 in switch I, and S41 side chain in the P-loop (Fig. 2b). This pattern of coordination is similar to that of the *in cis* arginine finger of human guanylate binding protein 1 (hGBP1)29 (Fig. 2c) and the bound potassium ion in the active site of MnmE (Fig. 2d), which mimics the function of an arginine finger28. We hypothesized that the sodium in our GG structure serves a similar purpose and indeed found that GTP hydrolysis in both GG (Supplementary Fig. 3b) and full-length dynamin (data not shown) is sensitive to the presence of different monovalent cations. Potassium, which is likely more physiologically relevant due to its higher intracellular concentration, induces a highesr hydrolysis rate than sodium, while rubidium and cesium impair turnover by increasing degrees.

The bound magnesium ion and K44 side chain also form hydrogen bonds with the β-phosphate and the aluminum fluoride (Fig. 2e). These interactions mirror the effects of the

sodium ion from the other side of the nucleotide and act in concert to stabilize the developing charge in the transition state. This explains the strong dominant-negative effects of dynamin(K44A), which is defective in both GTP binding and hydrolysis5,6.

The preponderance of backbone interactions in stabilizing the bridging and catalytic waters ($T65_O$, $G139_N$) and the bound cation ($G60_O$, $G62_O$) explains inabilities to define dynamin's basal catalytic mechanism by mutagenesis alone7,21,30. Previous studies7,30 have nonetheless identified S45, T65, T141, and K142 as important functional residues. Defects associated with these side chains can now be rationalized by our GG structure. S45 and T65 coordinate the bound magnesium, the disruption of which would prevent proper nucleotide binding and charge compensation. T141 in contrast does not actively contribute to the GG active site or the dimer interface, despite its location in switch II. However, substitutions at this position could sterically interfere with the *cis* and *trans* stabilizing loop interactions that restrict the conformational flexibility of switch II. Indeed, T141Q and T141D mutations have much stronger defects *in vitro* and *in vivo* than a smaller T141A substitution7,30. K142A moderately impairs dynamin GTP hydrolysis but strongly inhibits endocytosis30. K142 can hydrogen bond with E153 at the base of the GG dimer (Fig. 1e). Removal of this interaction could preferentially alter the dimerization-dependent functions of dynamin.

G domain conformational changes promote stimulated-hydrolysis

Superposition of GG with the rat dynamin GTPase domain (PDB: 2aka) reveals a number of significant conformational changes in the active site that prime dynamin for GTP hydrolysis (Fig. 3a). The P-loop tilts by ~55° as a result of GDP.AlF_4^- binding (Fig. 3b). This repositions Q40 and S41, allowing them to interact with the bridging water and the sodium ion respectively. The bound sodium engages switch I, which swings toward the nucleotide binding pocket (Fig. 3c). Nucleotide binding also restructures the extended DSL into a short α-helix. R237 mediates this rearrangement by flipping towards switch I to form the center of a dense hydrogen bond network that includes the E49, D55, and R59 side chains and the main chain atoms of F56, L57 and K240 (Fig. 3d, 3e). Many of these interactions are lost when only GDP is bound (Fig. 3f), as has also been observed in the dynamin A structure22 (PDB: 1jwy, Fig. 3f). This suggests that GTP hydrolysis and γ-phosphate release disengages switch I, which in turn would destabilize the conformation of the DSL to precipitate the break up of the dimer and allow GDP to dissociate. Additional movements in switch II and the *cis* stabilizing loop (residues 109–120) facilitate hydrogen bonding between N112 and D147 and the backbone carbonyl of K113 and Q148 *in cis* (Fig. 3g) to stabilize the conformation of switch II and maintain its orientation at the dimer interface.

Conserved catalytic machinery is required for function

Q40, S41, and D180 are absolutely conserved among dynamin family members (Fig. 4a) and are required for dynamin function *in vitro* and *in vivo*. Mutations of P-loop residues Q40 and S41 selectively impair stimulated GTP hydrolysis without significantly altering basal turnover (Fig. 4b, 4c, Supplemental Table 2). Mutants of Q40 produce the strongest defects, reducing the catalytic enhancement by ~80-fold, almost to the level of basal activity. As predicted from the structure, D180 mutations also selectively inhibit assembly-stimulated

GTPase activity (Fig. 4c). None of these substitutions affects dynamin's capacity for self-assembly (Supplementary Fig. 4), which is to be expected as self-assembly is nucleotide-independent4.

Dynamin is thought to play a dual role in clathrin-mediated endocytosis, such that basal activity is necessary for early endocytic events and assembly-stimulated activity is required in later stages for membrane fission1,17,18,31. The identification of mutations that selectively impair assembly-stimulated – but not basal – GTPase activity allowed us to establish directly the requirement for assembly-stimulated GTPase activity in membrane fission *in vivo*. For this we used an assay that measures late events in clathrin-mediated endocytosis: the internalization of transferrin conjugated to biotin via a cleavable disulfide bond (BSS-Tfn) into sealed vesicles that are inaccessible to a small membrane impermeant reducing agent (MesNa). Adenoviral-mediated overexpression of Q40E completely inhibits BSS-Tfn internalization (Fig. 4d). Importantly, as in dynamin knock-out cells32, fluid phase uptake is not affected (Fig. 4e), confirming the specificity of the inhibitory effects.

The BSE links the G domain to the stalk

The N_{GTPase}, C_{GTPase}, and C_{GED} termini form the bundle signaling element (BSE), a structure capable of modulating dynamin function *in vitro* and *in vivo*19. As predicted19–21, this element adopts a three-helix bundle configuration that buries an extensive, highly conserved hydrophobic surface (Fig. 5a). The BSE does not participate in GG dimerization and instead flanks the GTPase core of each GG monomer, protruding in opposite directions from the dimer axis. Structural comparison with the G domain from rat dynamin shows that the BSE can pivot as a rigid body around a conserved proline residue (P294) that kinks the C_{GTPase} helix (Fig. 5b, asterisk). The inter-helix angle between the C_{GTPase} segments on either side of P294 differs significantly in the two GG monomers of both the long (−68.8° vs. −53.4°) and short (−70.4° vs. −59.0°) axis crystal forms. Thus, while the G domains obey a non-crystallographic two fold symmetry strictly, the BSEs do so only approximately. This asymmetry indicates that the link between the G domain and the BSE is inherently flexible and susceptible to crystal-packing forces (Supplementary Fig. 5a). However, this flexibility is limited since the proline at the pivot point does not allow free variations of the relevant main chain dihedral angles. Conformational flexibility in this region has also been suggested by structures of the distantly related bacterial dynamin-like protein (BDLP)33. The functional significance of these observed variations is not yet known, though they may play a role in the conformational coupling of dynamin's GTPase and PH domains10,19,34.

Significantly, in both crystal forms, the BSE of one monomer is oriented nearly perpendicular to its partner in the other monomer (Fig. 1b, 5c, Supplementary Fig. 5b, 5c). Assuming that the connections between the BSE and the middle/GED stalk in full-length dynamin have at least some degree of rigidity, we would anticipate that the stalks protruding from the two monomers would also adopt a nearly perpendicular orientation. This orientation is incompatible with previous models for the assembled dynamin polymer where the G domains of adjacent dynamin subunits are positioned with the N_{GTPase} and C_{GTPase} helices perpendicular to the membrane surface (Supplementary Fig. 6a) and the stalks are assumed to extend toward the PH domains in a uniform, parallel array12,13,35. Subsequent

transition-state dimerization in this arrangement would require a significant rotation of the individual G domains relative to one another to achieve the orientation observed in the GG dimer (Supplementary Fig. 6b–e). This in turn would cause subunits in adjacent rungs of the polymer to rotate relative to each other (Fig. 5c).

Discussion

Our data establishes that G domain dimerization is an integral part of dynamin's assembly-stimulated GTPase activity. Dimerization stabilizes the conformations of the flexible switch regions and precipitates the dramatic enhancement of dynamin's basal activity by optimally positioning components of the catalytic machinery. This machinery, which includes Q40, S41 and D180, is absolutely conserved among classical dynamins but is absent in other large GTPases such as hGBP1 and BDLP (Fig. 4a). Though these proteins share some common functional characteristics with dynamins29,33, their catalytic machinery and mechanism of hydrolysis are distinctly different.

We predict that G domain dimerization occurs between two dynamin tetramers and not between subunits within a tetramer (Fig. 5d). Our GG dimer structure therefore reflects, at a minimum, the formation of a transition state-dependent dynamin octamer mediated by the association of G domains from two different tetramers (Fig. 5d). In solution, higher-ordered assemblies would be expected as each tetramer contains four independent G domains. Incubation of full-length dynamin with transition state mimics has shown this to be the case *in vitro*36, producing rings and spirals under physiological salt conditions in the absence of a lipid scaffold.

In vivo, dynamin assembles into 'collars' at the necks of deeply invaginated clathrin-coated pits to mediate membrane fission. Cryo-EM reconstructions of assembled dynamin in the nucleotide-free13 and GMPPCP-bound12 states have identified global conformational changes that can constrict the underlying membrane but not sever it. Paradoxically, mounting evidence suggests that stimulated GTP hydrolysis during dynamin-catalyzed membrane fission promotes disassembly of the dynamin collar8–11. Furthermore, long dynamin assemblies have been shown to inhibit fission8,11, indicating that this process depends on some dynamin detachment from the membrane surface. We speculate that the energy needed for this displacement comes from the transition state-dependent dimerization of dynamin's G domains. Given the relative orientation of the BSEs and the geometrical constraint imposed by G domain dimerization, this would require a rotation and/or displacement of adjacent tetramers leading to the asymmetric weakening of the PH domain-membrane interactions in one, or both, of the associated tetramers (Fig. 5d). Subsequent stimulated-hydrolysis would then dissociate the interacting G domains, releasing those dynamin subunits whose contact with the membrane has been weakened. Cycles of GTP binding, G domain dimerization, GTP hydrolysis and disassembly may be required to reach a critical size of the dynamin polymer to promote fission. Alternatively, one might imagine that G domain dimerization could twist and/or tilt adjacent membrane-associated dynamin subunits to generate additional curvature required for membrane fission.

These represent only the simplest models based on our current structural knowledge, and there are clearly other plausible alternatives. For example, it has also been proposed that GTP hydrolysis drives conformational changes to generate a mechanochemical power stroke that severs the membrane4,37–39. We cannot rule out the possibility that GTP hydrolysis causes additional force-generating conformational changes in dynamin that have yet to be identified. High-resolution structural studies examining full-length dynamin in different nucleotide states in combination with cryo-EM will be necessary to unravel these possibilities.

Methods Summary

Protein production, mutagenesis and biochemical assays of GG and full length dynamin were performed as previously described19,40. To isolate the GG dimer, purified GG monomer was incubated with 2 mM GDP, 2 mM $AlCl_3$, and 20 mM NaF for 30 minutes at 37°C in SEC buffer (20 mM Tris pH 8.0, 150 mM NaCl, 2 mM EGTA, 4 mM $MgCl_2$, and 1 mM DTT). The reaction mixture was then injected onto a Superdex 75 HR 10/30 column (GE Healthcare) to isolate dimeric species. Peak dimer fractions were pooled and concentrated to ~10 mg/ml. The GG dimer was crystallized by hanging drop vapor diffusion in 0.1M Tris pH 8.5, 25% PEG 3350, 200 mM NaCl, and 25–35% NaF using a drop size of 2–10 ml and a reservoir volume of 750 μl. Crystals grew in 4–5 days at either 17°C or 20°C. Crystals were frozen in liquid propane prior to data collection and required no additional cryo-protectant. Two orthorhombic crystal forms were obtained (Supplementary Table 1) that differed mainly in the length of their c axis: 175.7Å vs. 181.5Å, denoted "short axis" and "long axis" forms respectively. Both crystals contained a dimer of GG in their asymmetric unit. The long axis crystal form was solved with single isomorphous replacement with anomalous scattering (SIRAS) using SeMet GG crystals. The short axis crystal form was solved by molecular replacement using the refined long axis structure as a search model. See Supplementary Methods for more details.

Supplementary Material

Refer to Web version on PubMed Central for supplementary material.

Acknowledgements

We thank Vasyl Lukiyanchuk for assistance in cloning and purification, Alison Hickman, Joseph Mindell, and Rajesh Ramachandran for insightful discussions and technical advice, and Thomas Pucadyil and Rajesh Ramachandran for critical reading of the manuscript. We extend our gratitude to Jenny Hinshaw and Jason Mears for providing the unpublished coordinates for the GTPase docking model derived from their cryo-EM docking studies. We also thank Ray Stevens and Ian Wilson for structural advice, guidance, and the use of their laboratory facilities in the early stages of this work. This work was supported by NIH grants GM42455 and MH61345 to SLS and the Intramural Program of the National Institute of Diabetes, Digestive, and Kidney Diseases (NIDDK) of the NIH. JSC was supported by a Ruth Kirschstein individual predoctoral fellowship from the NIMH (MH081419) and by a postdoctoral Intramural Research Training Award from NIDDK. Data were collected at the SER-CAT 22-ID beamline at the Advanced Photon Source, Argonne National Laboratory. Use of the APS was supported by the US Department of Energy, Basic Energy Sciences, Office of Science, under Contract No. W-31-109-Eng-38.

References

1. Mettlen M, Pucadyil TJ, Ramachandran R, Schmid SL. Dissecting dynamin’s role in clathrin-mediated endocytosis. Bioc. Soc. Trans. 2009; 37:1022–1026.

2. Praefcke GJ, McMahon HT. The dynamin superfamily: universal membrane tubulation and fission molecules? Nat. Rev. Mol. Cell Biol. 2004; 5:133–147. [PubMed: 15040446]
3. Muhlberg AB, Warnock DE, Schmid SL. Domain structure and intramolecular regulation of dynamin GTPase. EMBO J. 1997; 16:6676–6683. [PubMed: 9362482]
4. Stowell MH, Marks B, Wigge P, McMahon HT. Nucleotide-dependent conformational changes in dynamin: evidence for a mechanochemical molecular spring. Nat. Cell Biol. 1999; 1:27–32. [PubMed: 10559860]
5. Damke H, Baba T, Warnock DE, Schmid SL. Induction of mutant dynamin specifically blocks endocytic coated vesicle formation. J. Cell Biol. 1994; 127:915–934. [PubMed: 7962076]
6. Damke H, Binns DD, Ueda H, Schmid SL, Baba T. Dynamin GTPase domain mutants block endocytic vesicle formation at morphologically distinct stages. Mol. Biol. Cell. 2001; 12:2578–2589. [PubMed: 11553700]
7. Song BD, Leonard M, Schmid SL. Dynamin GTPase domain mutants that differentially affect GTP binding, GTP hydrolysis, and clathrin-mediated endocytosis. J. Biol. Chem. 2004; 279:40431–40436. [PubMed: 15262989]
8. Pucadyil TJ, Schmid SL. Real-time visualization of dynamin-catalyzed membrane fission and vesicle release. Cell. 2008; 135:1263–1275. [PubMed: 19084268]
9. Danino D, Moon KH, Hinshaw JE. Rapid constriction of lipid bilayers by the mechanochemical enzyme dynamin. J. Struct. Biol. 2004; 147:259–267. [PubMed: 15450295]
10. Ramachandran R, Schmid SL. Real-time detection reveals that effectors couple dynamin's GTP-dependent conformational changes to the membrane. EMBO J. 2008; 27:27–37. [PubMed: 18079695]
11. Bashkirov PV, et al. GTPase cycle of dynamin is coupled to membrane squeeze and release, leading to spontaneous fission. Cell. 2008; 135:1276–1286. [PubMed: 19084269]
12. Zhang P, Hinshaw JE. Three-dimensional reconstruction of dynamin in the constricted state. Nat. Cell Biol. 2001; 3:922–926. [PubMed: 11584275]
13. Chen YJ, Zhang P, Egelman EH, Hinshaw JE. The stalk region of dynamin drives the constriction of dynamin tubes. Nat. Struct. Mol. Biol. 2004; 11:574–575. [PubMed: 15133500]
14. Song BD, Yarar D, Schmid SL. An assembly-incompetent mutant establishes a requirement for dynamin self-assembly in clathrin-mediated endocytosis in vivo. Mol. Biol. Cell. 2004; 15:2243–2252. [PubMed: 15004222]
15. Sever S, et al. Physical and functional connection between auxilin and dynamin during endocytosis. EMBO J. 2006; 25:4163–4174. [PubMed: 16946707]
16. Ramachandran, et al. The dynamin middle domain is critical for tetramerization and higher-order self-assembly. EMBO J. 2007; 26:559–566. [PubMed: 17170701]
17. Sever S, Muhlberg AB, Schmid SL. Impairment of dynamin's GAP domain stimulates receptor-mediated endocytosis. Nature. 1999; 398:481–486. [PubMed: 10206643]
18. Narayanan R, Leonard M, Song BD, Schmid SL, Ramaswami M. An internal GAP domain negatively regulates presynaptic dynamin in vivo: a two-step model for dynamin function. J. Cell Biol. 2005; 169:117–126. [PubMed: 15824135]
19. Chappie JS, et al. An intramolecular signaling element that modulates dynamin function in vitro and in vivo. Mol. Biol. Cell. 2009; 20:3561–3571. [PubMed: 19515832]
20. Smirnova E, Shurland DL, Newman-Smith ED, Pishvaee B, van der Bliek AM. A model for dynamin self-assembly based on binding between three different protein domains. J. Biol. Chem. 1999; 274:14942–14947. [PubMed: 10329695]
21. Reubold TF, et al. Crystal structure of the GTPase domain of rat dynamin 1. Proc. Natl. Acad. Sci. USA. 2005; 102:13093–13098. [PubMed: 16141317]
22. Niemann HH, Knetsch MLW, Scherer A, Manstein DJ, Kull FJ. Crystal structure of a dynamin GTPase domain in both nucleotide-free and GDP-bound forms. EMBO J. 2001; 20:5813–5821. [PubMed: 11689422]
23. Bourne HR, Sanders DA, McCormick F. The GTPase superfamily: conserved structure and molecular mechanism. Nature. 1991; 349:117–127. [PubMed: 1898771]

24. Li G, Zhang XC. GTP hydrolysis mechanism of Ras-like GTPases. J. Mol. Biol. 2004; 340:921–932. [PubMed: 15236956]
25. Scheffzek K, Ahmadian MR, Wittinghofer A. GTPase-activating proteins: helping hands to complement an active site. Trends Biochem. Sci. 1998; 23:257–262. [PubMed: 9697416]
26. Tesmer JJG, Berman DM, Gilman AG, Sprang SR. Structure of RGS4 bound to AlF_4^--activated Giα1: stabilization of the transition state for GTP hydrolysis. Cell. 1997; 89:251–261. [PubMed: 9108480]
27. Gasper R, Meyer S, Gotthardt K, Sirajuddin M, Wittinghofer A. It takes two to tango: regulation of G proteins by dimerization. Nat. Rev. Mol. Cell Biol. 2009; 10:423–429. [PubMed: 19424291]
28. Scrima A, Wittinghofer A. Dimerisation-dependent GTPase reaction of MnmE: how potassium acts as GTPase-activating element. EMBO J. 2006; 25:2940–2951. [PubMed: 16763562]
29. Ghosh A, Praefcke GJ, Renault L, Wittinghofer A, Herrmann C. How guanylate-binding proteins achieve assembly-stimulated processive cleavage of GTP to GMP. Nature. 2006; 440:101–104. [PubMed: 16511497]
30. Marks B, et al. GTPase activity of dynamin and resulting conformation change are essential for endocytosis. Nature. 2001; 410:231–235. [PubMed: 11242086]
31. Loerke D, et al. Cargo and dynamin regulate clathrin-coated pit maturation. PLoS Biol. 2009; 7:e57. [PubMed: 19296720]
32. Ferguson S, et al. Coordinated actions of actin and BAR proteins upstream of dynamin at endocytic clathrin-coated pits. Dev. Cell. 2009; 17:811–822. [PubMed: 20059951]
33. Low HH, Sachse C, Amos LA, Lowe J. Structure of a bacterial dynamin-like protein lipid tube provides a mechanism for assembly and membrane curving. Cell. 2009; 139:1342–1352. [PubMed: 20064379]
34. Solomaha E, Palfrey HC. Conformational changes in dynamin on GTP binding and oligomerization reported by intrinsic and extrinsic fluorescence. Biochem. J. 2005; 391:601–611. [PubMed: 15954862]
35. Mears JA, Ray P, Hinshaw JE. A corkscrew model for dynamin constriction. Structure. 2007; 15:1190–1202. [PubMed: 17937909]
36. Carr JF, Hinshaw JE. Dynamin assembles into spirals under physiological salt conditions upon the addition of GDP and gamma-phosphate analogues. J. Biol. Chem. 1997; 272:28030–28035. [PubMed: 9346955]
37. Hinshaw JE, Schmid SL. Dynamin self-assembles into rings suggesting a mechanism for coated vesicle budding. Nature. 1995; 374:190–192. [PubMed: 7877694]
38. Sweitzer SM, Hinshaw JE. Dynamin undergoes a GTP-dependent conformational change causing vesiculation. Cell. 1998; 93:1021–1029. [PubMed: 9635431]
39. Roux A, Uyhazi K, Frost A, De Camilli P. GTP-dependent twisting of dynamin implicates constriction and tension in membrane fission. Nature. 2006; 441:528–531. [PubMed: 16648839]
40. Leonard M, Song BD, Ramachandran R, Schimd SL. Robust colorimetric assays for dynamin's basal and stimulated GTPase activities. Meth. Enzymol. 2005; 404:490–503. [PubMed: 16413294]

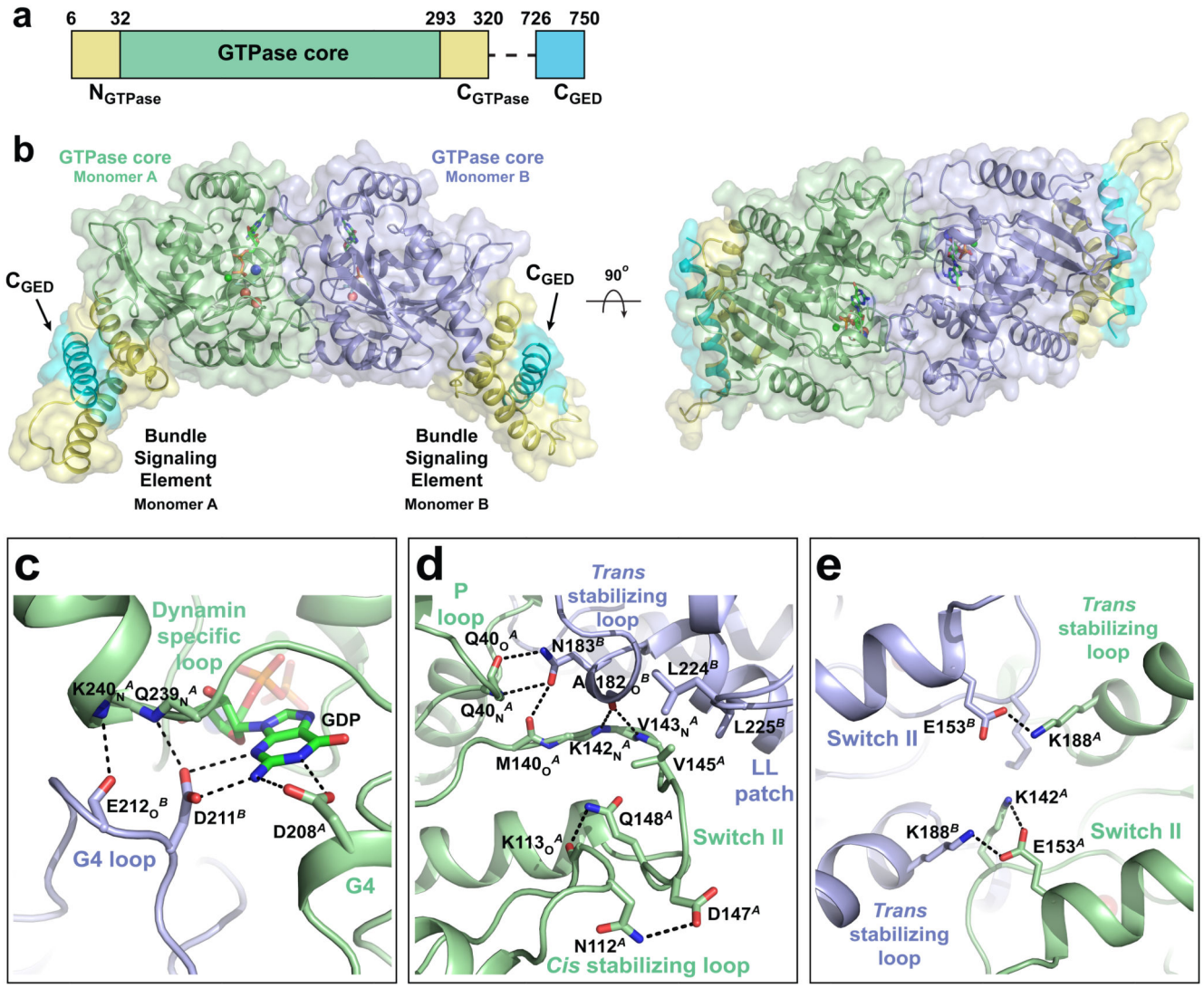

Fig. 1. Structure of GG dimer

a, Domain arrangement of GTPase-GED (GG) fusion constructed from human dynamin 1. Each monomer contains a GTPase core (green) and three helical segments: N_{GTPase}, C_{GTPase} (yellow) and C_{GED} (cyan). Dashed line denotes the flexible linker that tethers the C_{GED} helix. b, Structure of GDP.AlF_4^--stabilized GG dimer from the "long axis" crystal form shown from the side (left) and top (right). The GTPase cores of individual monomers are colored in green and blue. The helical segments in each monomer that constitute the bundle signaling element (BSE) are colored yellow with the C_{GED} helix highlighted in cyan. c, d, e, Structural interactions that stabilize the GG dimer. Coloring is the same as b. Key residues are labeled with a superscript (A or B) to indicate from which monomer they originate. The additional subscript (O or N) signifies the interaction of a main chain carbonyl or nitrogen. Dashed lines indicate hydrogen-bonding interactions.

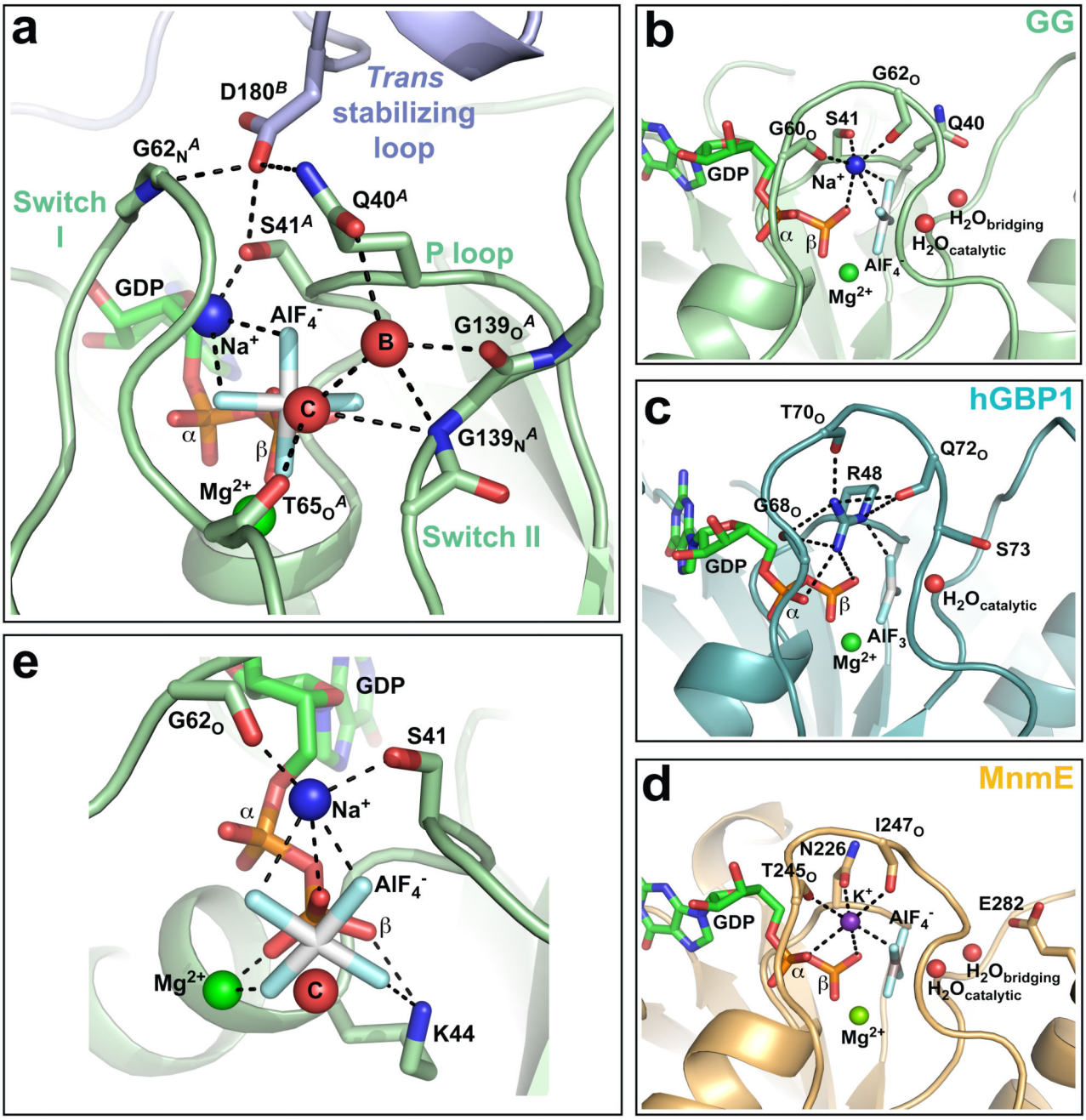

Fig. 2. Catalytic machinery involved in dynamin GTP hydrolysis

a, Structure of GG active site. Red spheres labelled “C” and “B” denote catalytic and bridging waters respectively. Dashed lines indicate hydrogen-bonding interactions. b–d, Comparison of the charge-compensating elements in GG (b), hGBP1 (PDB: 2b92) (c), and MnmE (PDB: 2gj8) (d). Note the similar coordination by switch I in each case. e, K44 and the bound magnesium form similar charge-compensating interactions with the β-phosphate and aluminum fluoride. Portions of switch I and switch II have been removed for clarity. Red sphere labeled “C” denotes the catalytic water.

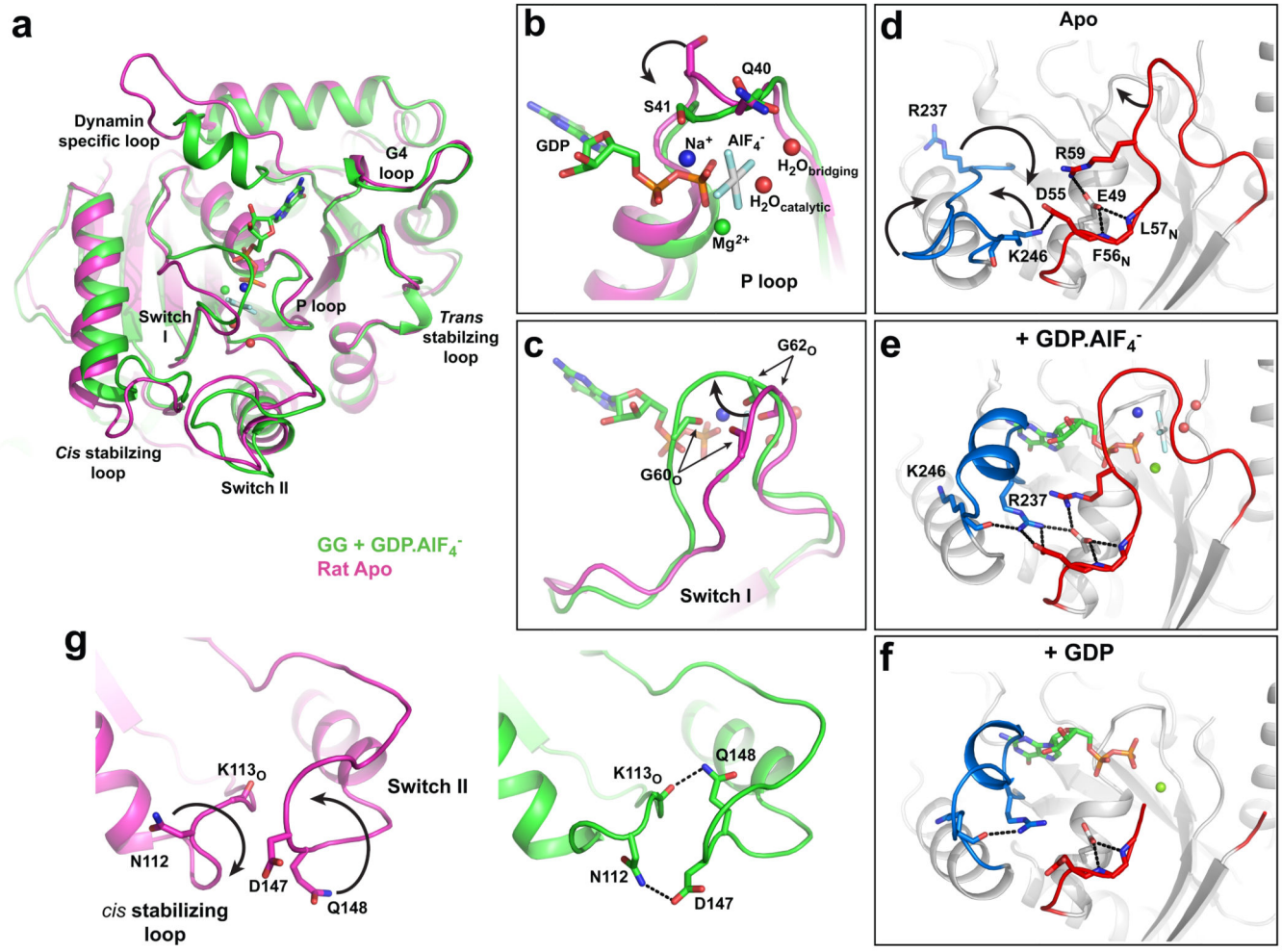

Fig. 3. Active site conformational changes induced by dynamin G-domain dimerization and GTP hydrolysis

a, A monomer from the GG dimer structure (green) is superimposed with the nucleotide free rat dynamin G domain structure (magenta, PDB: 2aka). The GDP.AlF_4^-, magnesium, and active site waters from GG structure are shown. Coloring is the same in b, c, and g. Black arrows indicate structural movements induced by nucleotide binding and dimerization. b, P-loop tilting reorients Q40 and S41 to facilitate interactions with the bridging water and sodium ion respectively. c, GTP binding engages switch I, resulting in the coordination of the charge-compensating cation by the backbone carbonyl oxygens of G60 and G62. d–f, Conformational changes of the dynamin specific loop (colored blue) are mediated by a dense network of hydrogen bonding that includes switch I residues (red), as shown for d, nucleotide free rat dynamin GTPase domain (c, PDB: 2aka); e, GDP.AlF4--stabilized GG dimer (d, long axis crystal form), and f, GDP-bound Dictyostelium dynamin A (e, PDB: 1jwy). g, Switch II and the *cis* stabilizing loop undergo significant conformational rearrangements that precipitate hydrogen bonding between N112 and D147 and between the K113 carbonyl oxygen and Q148. These interactions stabilize switch II *in cis*, whereas

interactions with the *trans* stabilizing loop across the dimer interface stabilize switch II *in trans*.

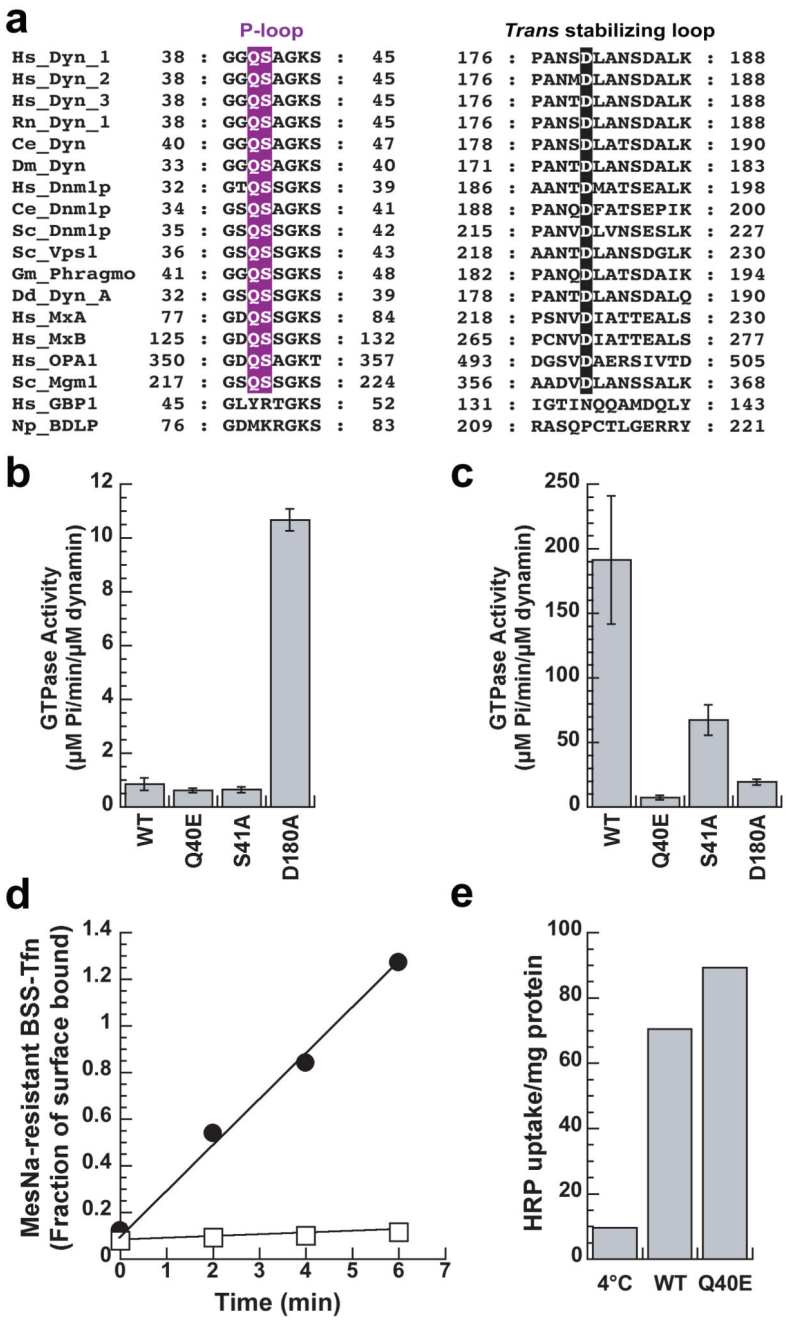

Fig. 4. Functional analyses of dynamin active site mutants

A, Q40, S41, and D180 are absolutely conserved among dynamin family members, but not more distantly related GTPases. Sequence alignment abbreviations are as follows: Hs, *Homo sapiens*; Rn, *Rattus norvegicus*; Dm, *Drosophila melanogaster*; Ce, *Caenorhabditis elegans*; Sc, *Saccharomyces cerevisiae*; Dd, *Dictyostelium discoideum*; Dyn, dynamin; Gm_Phragmo, *Glycine max* phragmoplastin; Hs_GBP1, interferon-γ-induced human guanylate binding protein; Np_BDLP, *Nostoc punctiforme* bacterial dynamin-like protein. b, Basal and c, assembly-stimulated GTPase activities of full-length wildtype and dynamin

active site mutants (Q40E, S41A, and D180A) were determined as described in Methods. These data represent the average of at least three independent experiments with multiple independently purified batches of protein. d, Clathrin-mediated internalization of BSS-Tfn into MesNa-inaccessessible sealed vesicles and e, fluid-phase uptake of horse radish peroxidase into tTA-HeLa cells infected with adenoviruses expressing either WT or Q40E dynamin-1.

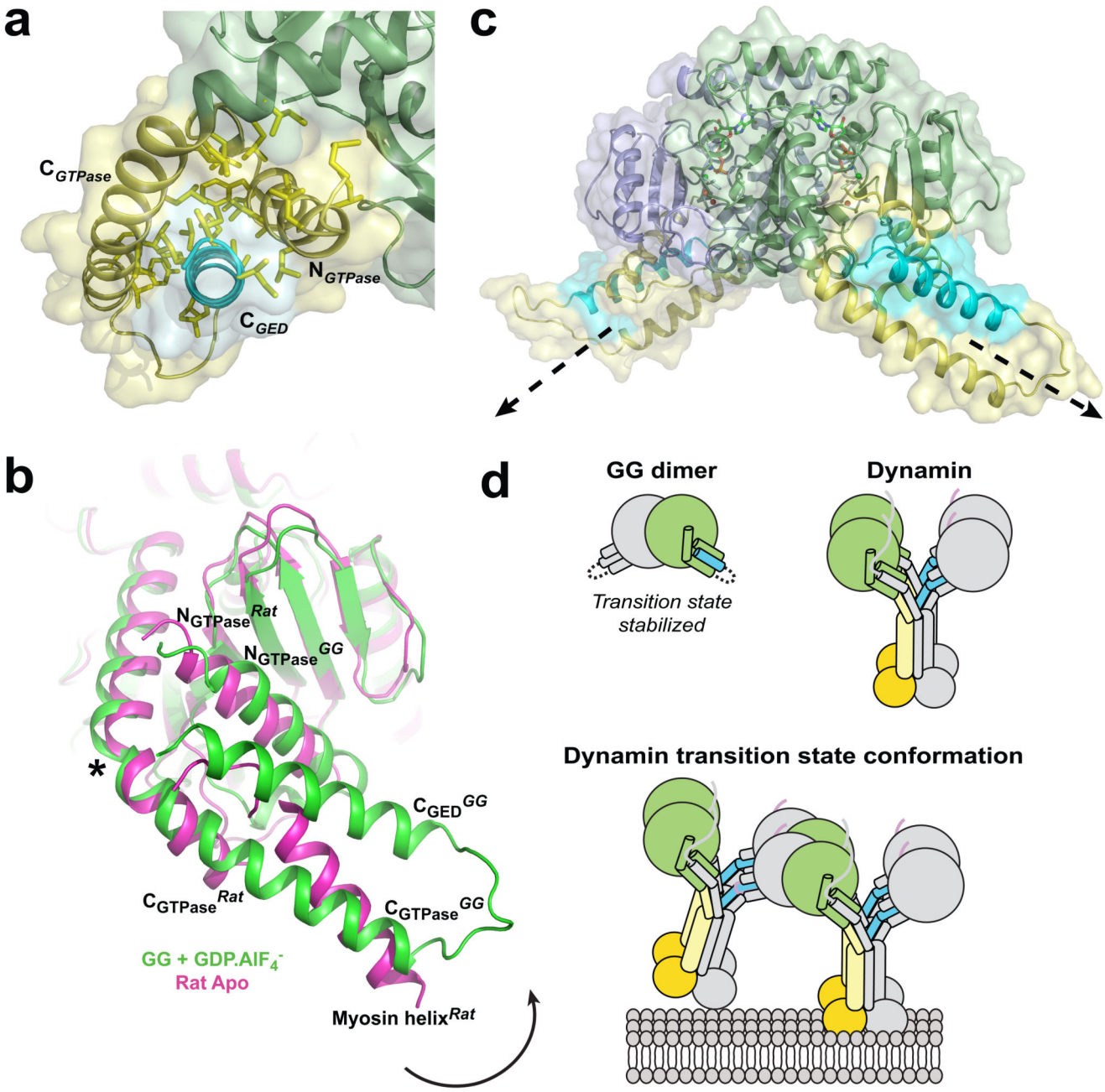

Fig. 5. Structure and conformational changes of the BSE

a, The BSE as viewed down the C_{GED} helix. Conserved hydrophobic side chains that comprise the GTPase-GED interface are shown in yellow. b, BSE conformational changes. Superposition shows a monomer from the GG dimer structure (green) superimposed with the nucleotide free rat dynamin G domain structure (PDB: 2aka, magenta). Black arrow indicates relative movement of BSE upon GTP hydrolysis. Asterisk denotes the position of conserved P294 that kinks the C_{GTPase} segment. A helix from the fused myosin motor domain mimics the C_{GED} segment in the rat dynamin structure. c, Relative orientation of the BSEs in the GG dimer. Structure is rotated 120° about the y-axis from the side view

depicted in Fig. 1b. Dashed arrows indicate the assumed position of the middle/GED stalk in each monomer that is connected to the BSE in full-length dynamin. **d**, Cartoon illustrating C_{GED}'s association with the GTPase domain in GG and full-length dynamin. In GG, this interaction occurs *in cis*, producing a stable monomer that dimerizes only in the presence of a transition state mimic; in the full-length dynamin, C_{GED} interacts with the GTPase domain *in trans*, producing a stable dimer that associates further via middle/GED stalk interactions to form the tetramer. The transition state conformation of a membrane-bound minimal dynamin octamer as predicted from the GG dimer structure is also shown.